Electronic Supplementary Material (ESI) for Organic & Biomolecular Chemistry.

Supporting Information

Structure–property relationships of photoresponsive inhibitors of the kinesin motor

Ammathnadu S. Amrutha, K. R. Sunil Kumar, Kazuya Matsuo, Nobuyuki Tamaoki*

Research Institute for Electronic science, Hokkaido University, N20, W10, Kita-Ku, Sapporo-001-0020, Hokkaido, Japan

*Corresponding author:
E-mail: tamaoki@es.hokudai.ac.jp

Phone: +81-11-706-9356

Table of contents

1. Mass spectra of azo-peptides

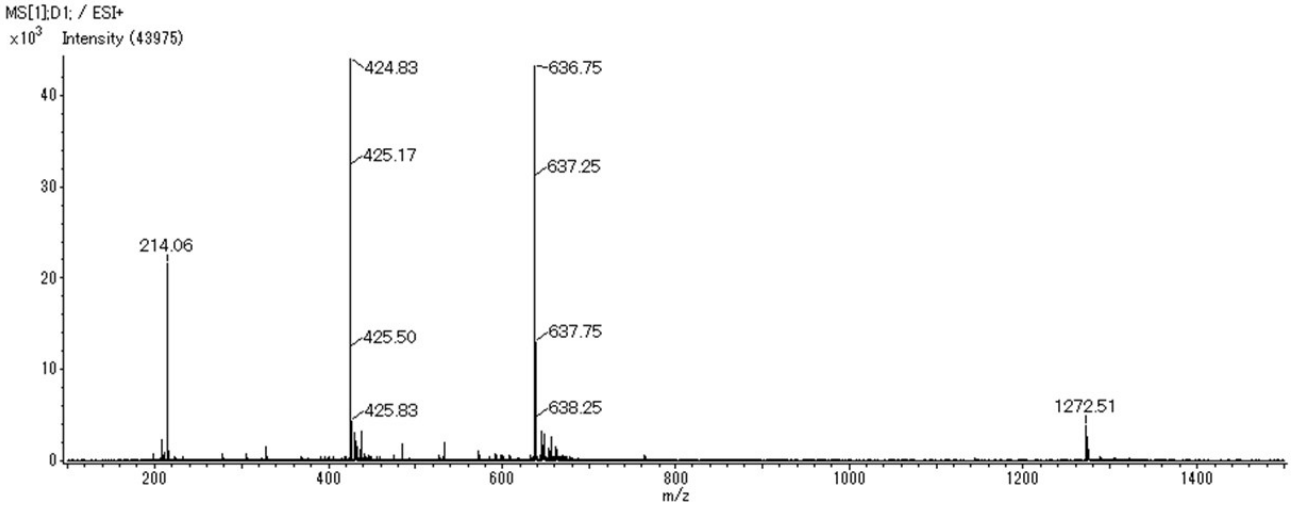

Figure S1. ESI$^+$ mass spectrum of azo-peptide **2**: m/z = 1272.51 $[M+H]^+$ (calculated mass for the most abundant isotope: 1272.65)

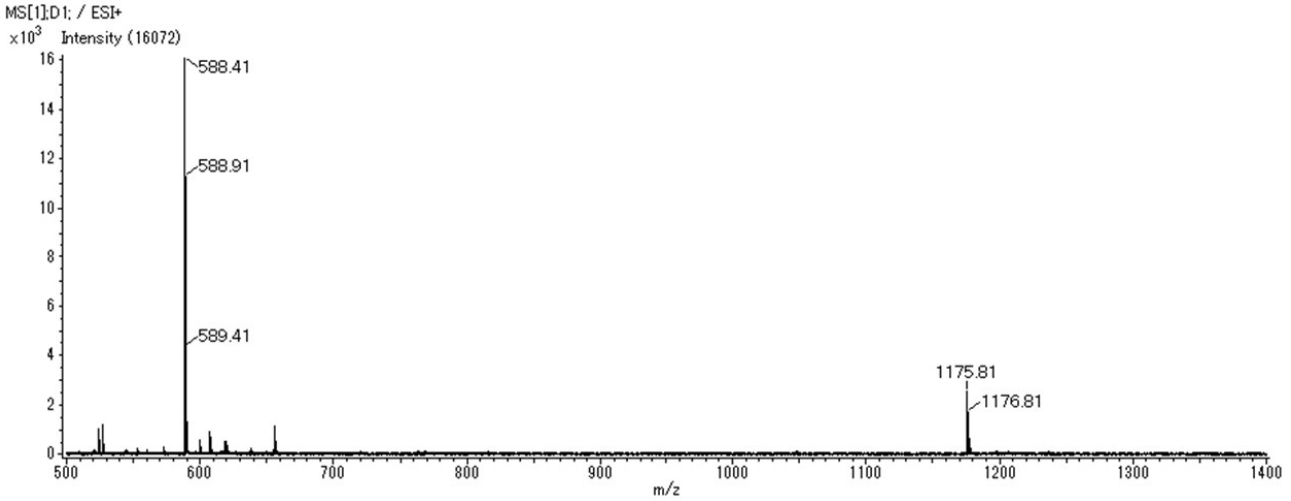

Figure S2. ESI$^+$ mass spectrum of azo-peptide **3**: m/z = 1175.81 $[M+H]^+$ (calculated mass for the most abundant isotope: 1175.6)

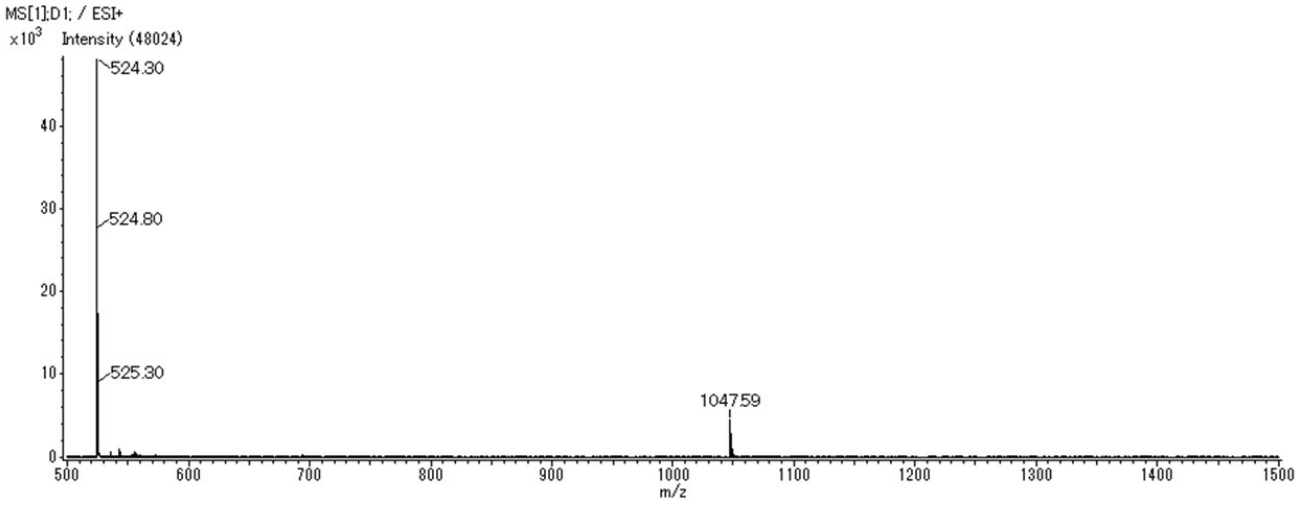

Figure S3. ESI$^+$ mass spectrum of azo-peptide **4**: m/z = 1047.59 $[M+H]^+$ (calculated mass for the most abundant isotope: 1047.50)

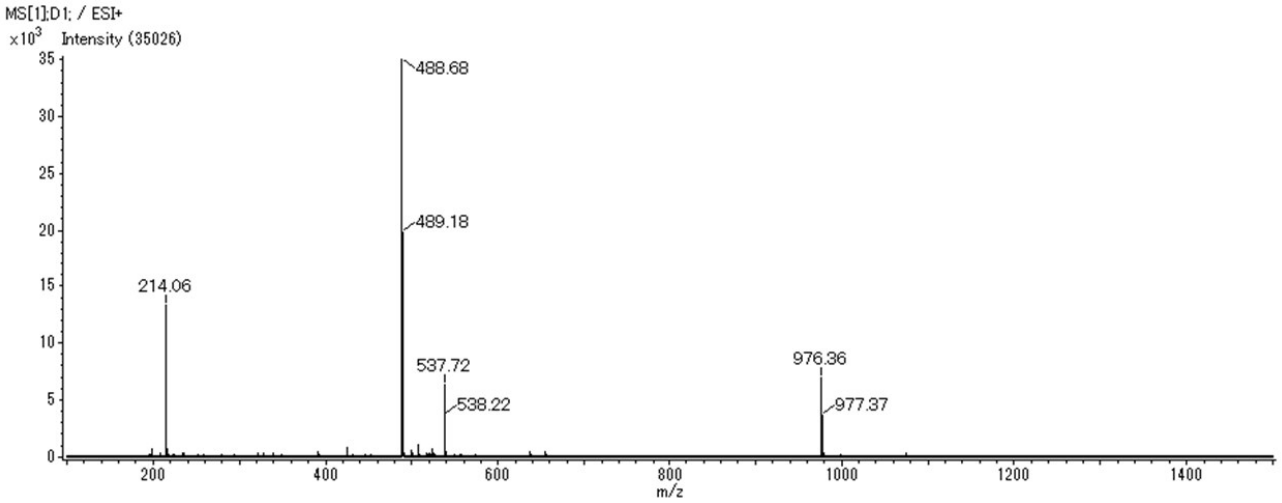

Figure S4. ESI$^+$ mass spectrum of azo-peptide **5**: m/z = 976.36 $[M+H]^+$ (calculated mass for the most abundant isotope: 976.47)

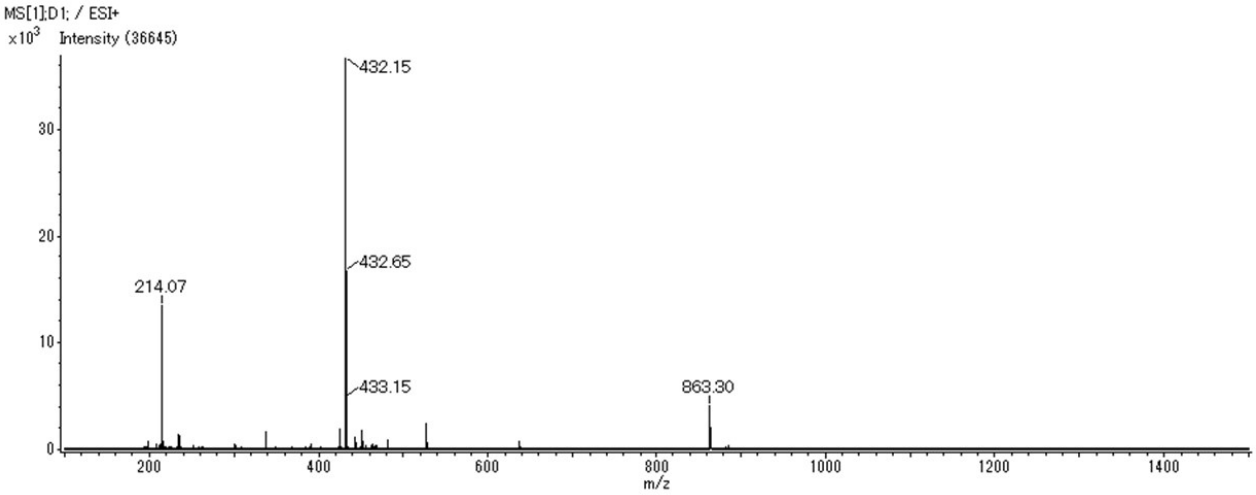

Figure S5. ESI$^+$ mass spectrum of azo-peptide **6**: m/z = 863.30 $[M+H]^+$ (calculated mass for the most abundant isotope: 863.38)

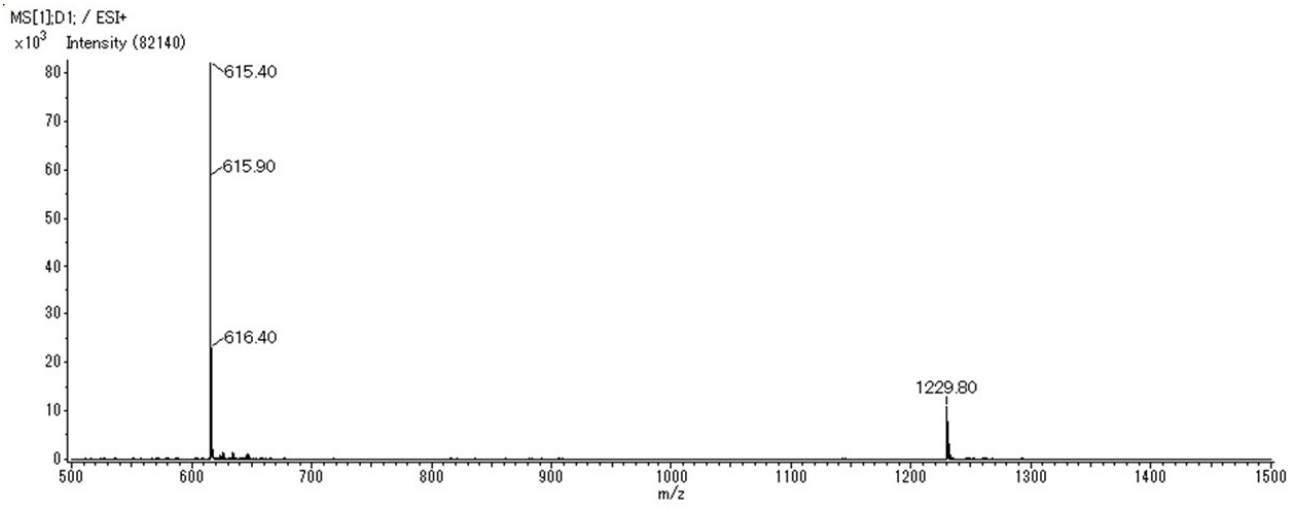

Figure S6. ESI$^+$ mass spectrum of azo-peptide **7**: m/z = 1229.80 $[M+H]^+$ (calculated mass for the most abundant isotope: 1229.64)

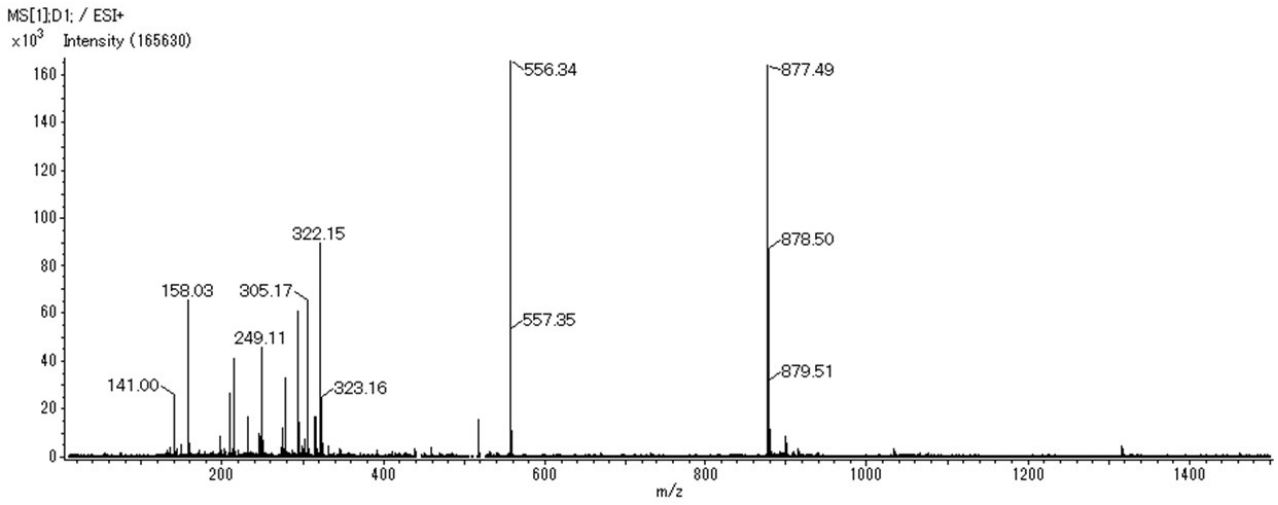

Figure S7. ESI$^+$ mass spectrum of azo-peptide **8**: m/z = 877.49 $[M+H]^+$ (calculated mass for the most abundant isotope: 877.49), m/z = 556.34 $[Pro\text{-}Lys\text{-}Ala\text{-}Ile\text{-}Gln+H]^+$and 322.15 $[Azo\text{-}Ile]^+$ (calculated mass for the fragments of the parent azo-peptide **8** cleaved at the amide linkage between the Ile and Pro : 556.34 and 322.15 respectively)

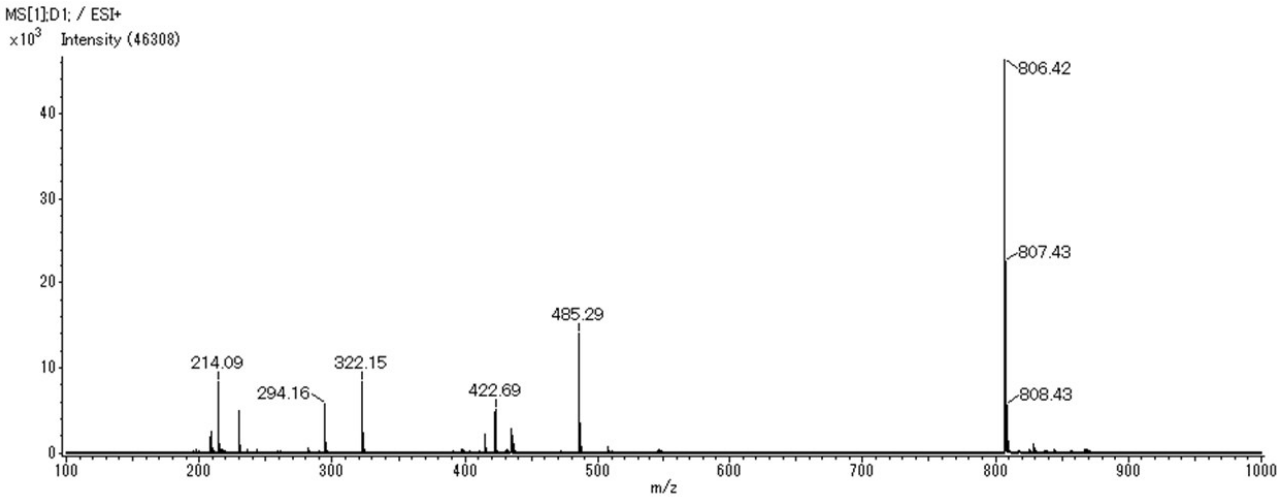

Figure S8. ESI$^+$ mass spectrum of azo-peptide **9**: m/z = 806.42 $[M+H]^+$ (calculated mass for the most abundant isotope: 806.45), m/z = 485.29 $[Pro\text{-}Lys\text{-}Ala\text{-}Ile\text{-}Gly+H]^+$and 322.15 $[Azo\text{-}Ile]^+$ (calculated mass for the fragments of the parent azo-peptide **9** cleaved at the amide linkage between the Ile and Pro : 485.30 and 322.15 respectively), m/z = 422.69 $[M+H+K]^{2+}$ (calculated mass for the most abundant isotope: 422.77).

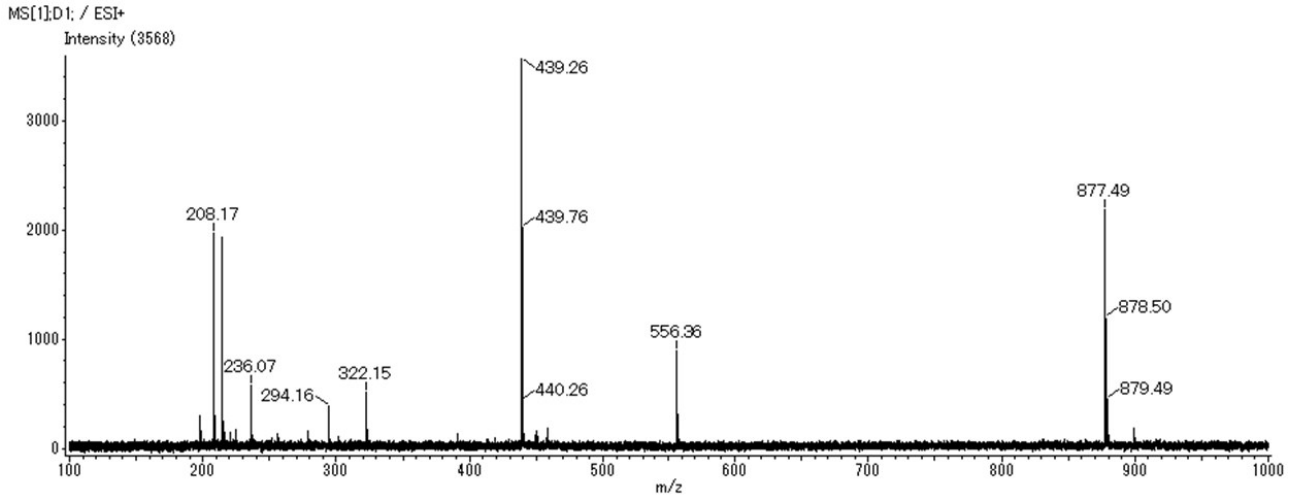

Figure S9. ESI⁺ mass spectrum of azo-peptide **10**: m/z = 877.49 $[M+H]^+$ (calculated mass for the most abundant isotope: 877.52)

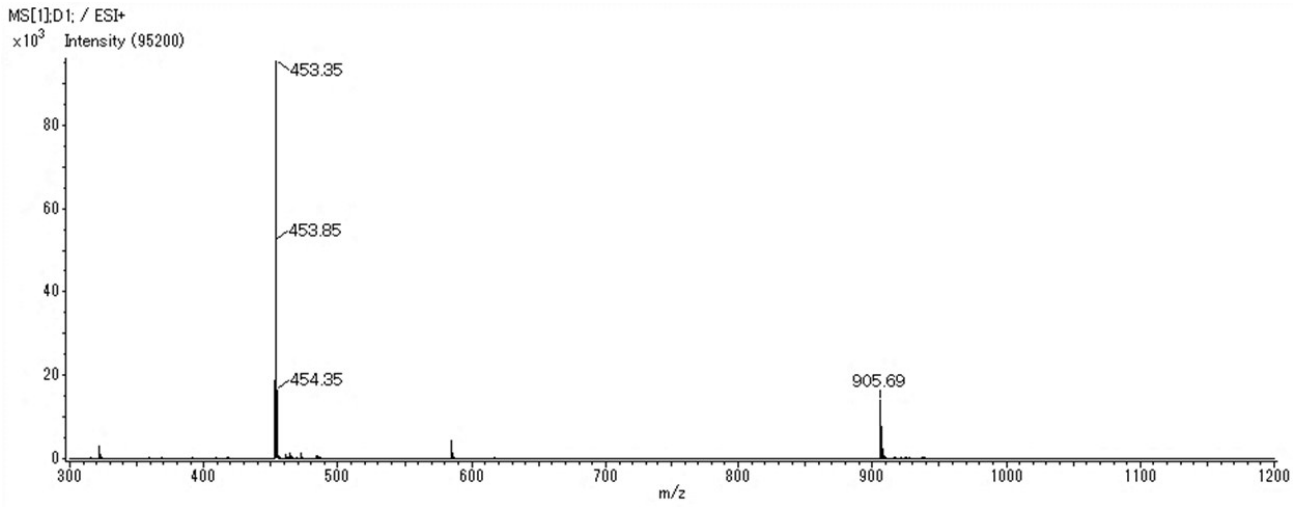

Figure S10. ESI⁺ mass spectrum of azo-peptide **11**: m/z = 905.69 $[M+H]^+$ (calculated mass for the most abundant isotope: 905.53)

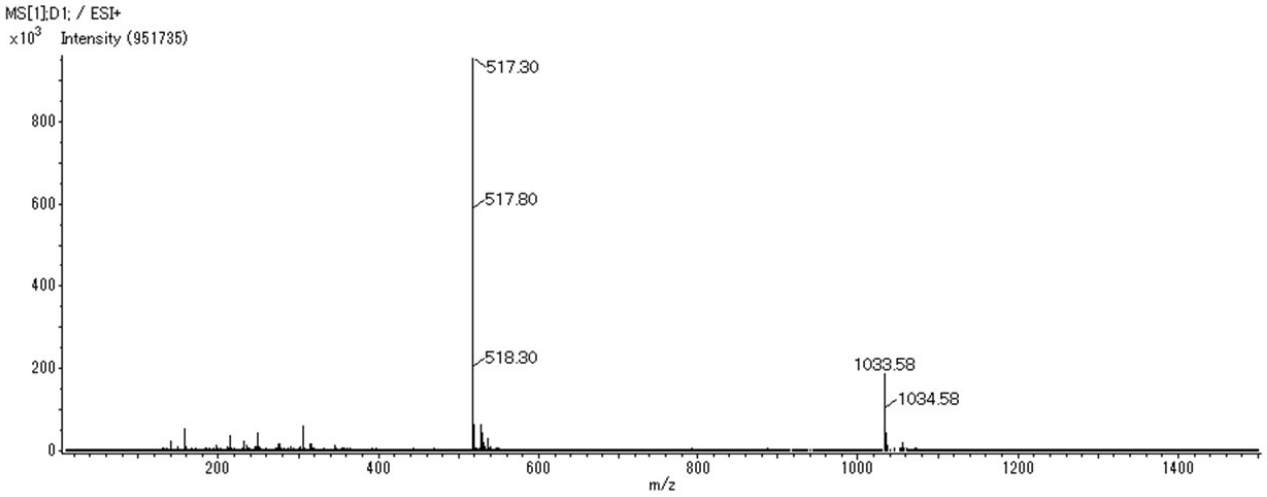

Figure S11. ESI$^+$ mass spectrum of azo-peptide **12**: m/z = 1033.58 $[M+H]^+$ (calculated mass for the most abundant isotope: 1033.59)

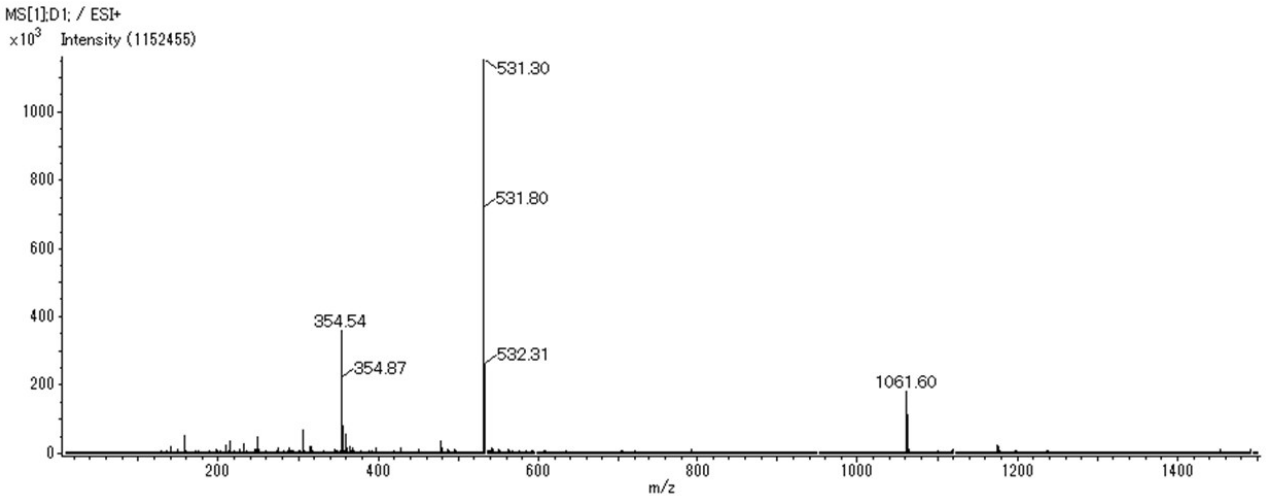

Figure S12. ESI$^+$ mass spectrum of azo-peptide **13**: m/z = 1061.60 $[M+H]^+$ (calculated mass for the most abundant isotope: 1061.63)

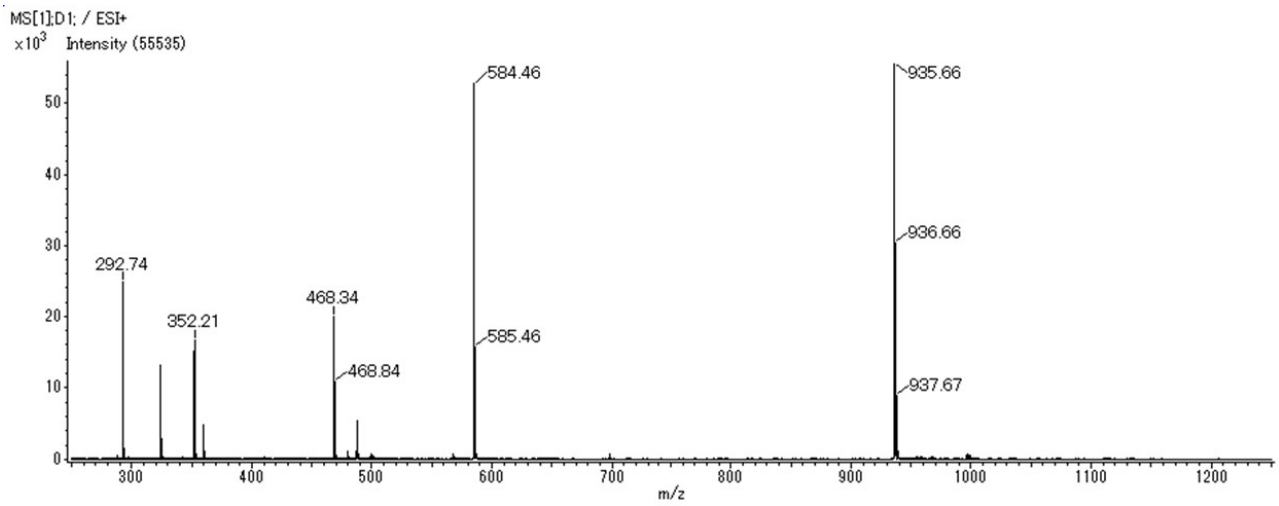

Figure S13. ESI$^+$ mass spectrum of azo-peptide **14**: m/z = 935.66 $[M+H]^+$ (calculated mass for the most abundant isotope: 935.54), m/z = 584.46 [Pro-Lys-Ala-Ile-Arg+H]$^+$and 352.21 $[MeO\text{-}Azo\text{-}Ile]^+$ (calculated mass for the fragments of the parent azo-peptide **14** cleaved at the amide linkage between the Ile and Pro : 584.38 and 352.16 respectively), m/z = 468.34 $[M+2H]^{2+}$ (calculated mass for the most abundant isotope: 468.27).

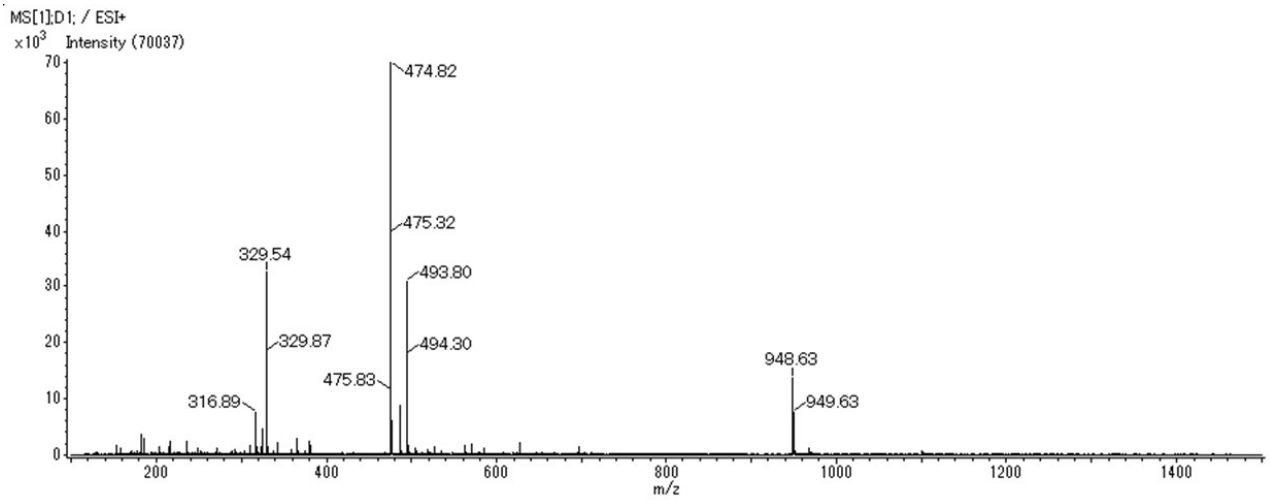

Figure S14. ESI$^+$ mass spectrum of azo-peptide **15**: m/z = 948.63 $[M+H]^+$ (calculated mass for the most abundant isotope: 948.57)

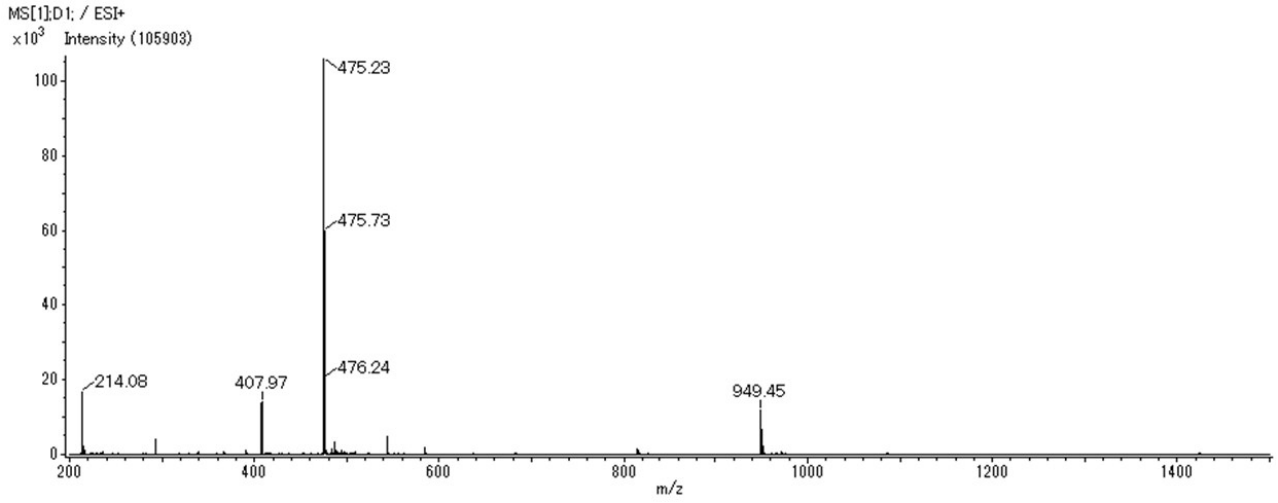

Figure S15. ESI^+ mass spectrum of azo-peptide **16**: m/z = 949.45 $[M+H]^+$ (calculated mass for the most abundant isotope: 949.52)

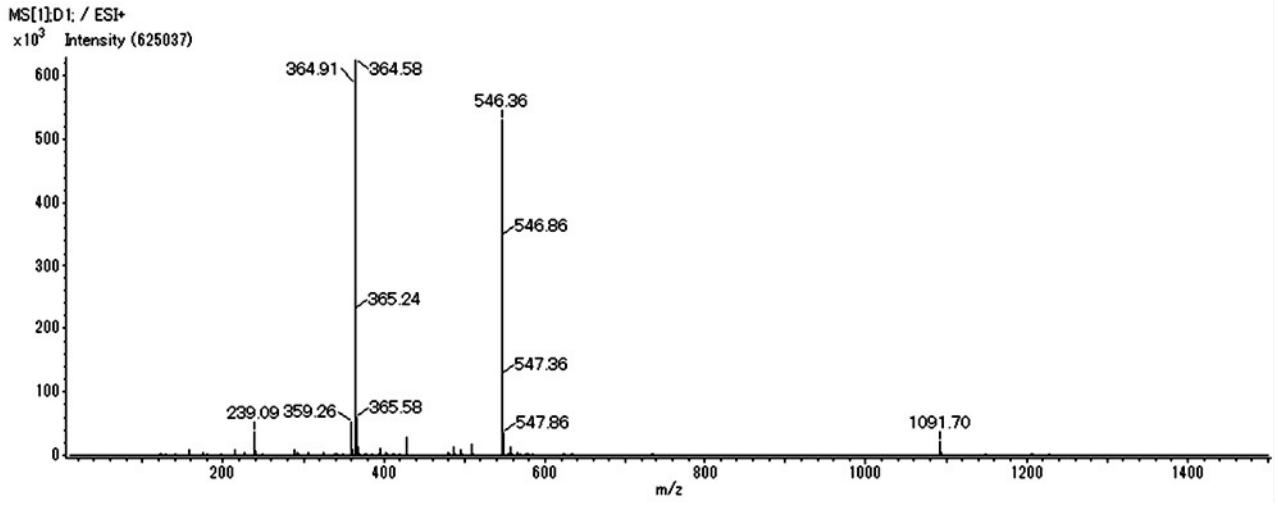

Figure S16. ESI^+ mass spectrum of azo-peptide **17**: m/z = 1091.70 $[M+H]^+$ (calculated mass for the most abundant isotope: 1091.64)

2. Purity of the azo-peptides by HPLC analysis

(a) azo-peptide **2**

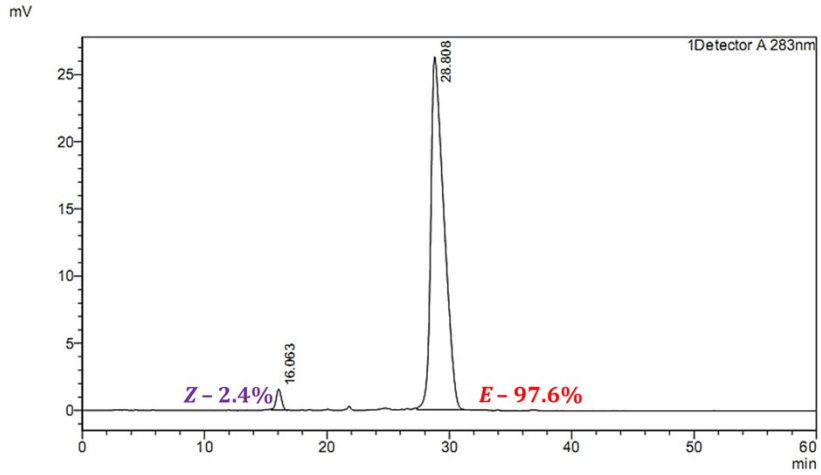

(b) azo-peptide **3**

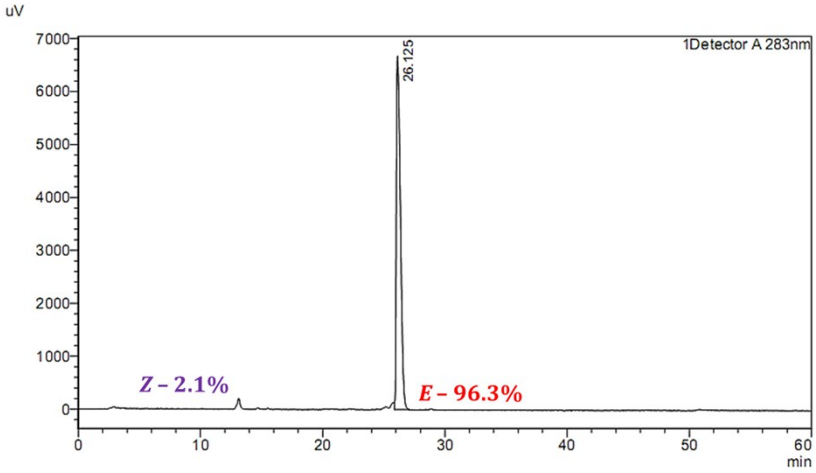

(c) azo-peptide **4**

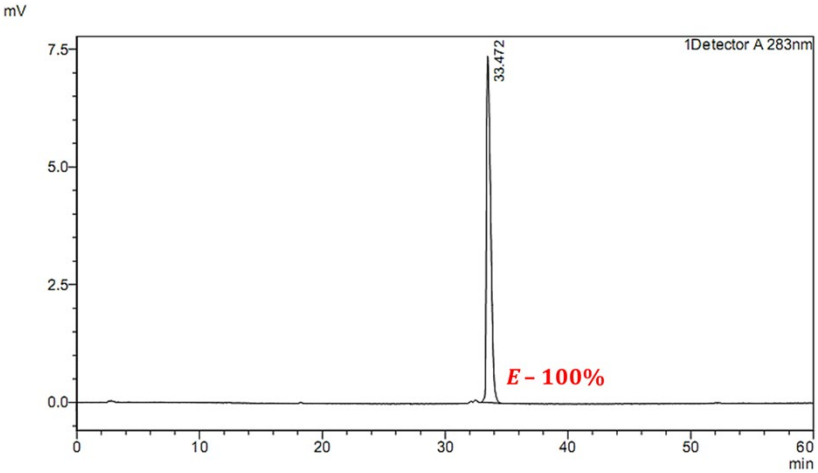

(d) azo-peptide **5**

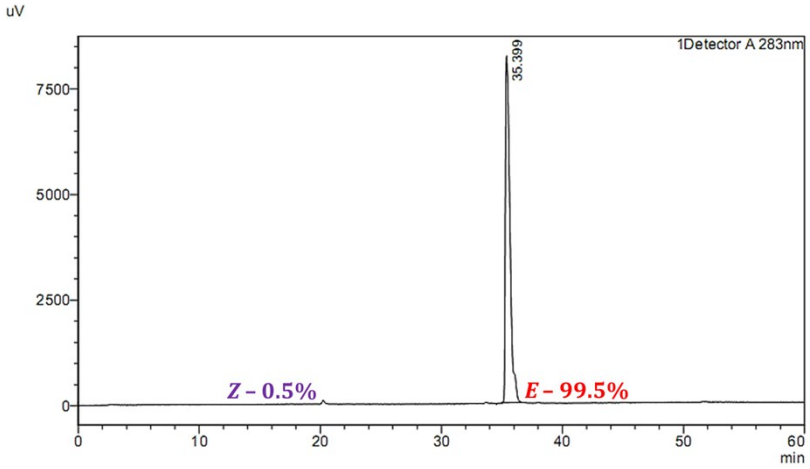

(e) azo-peptide **6**

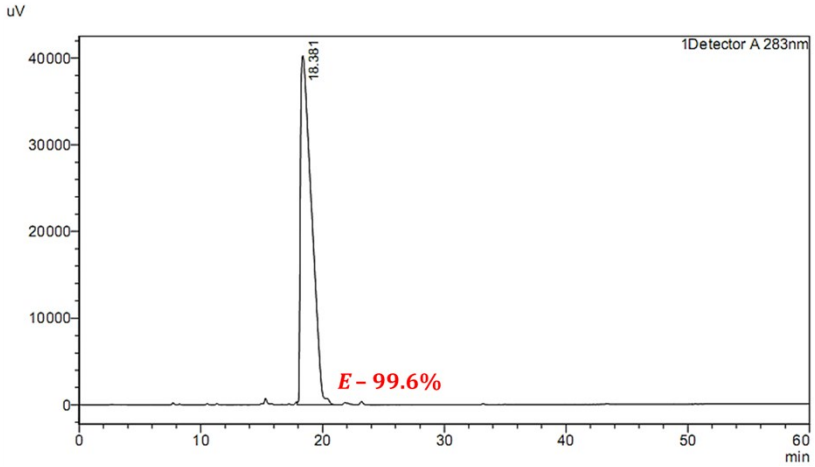

(f) azo-peptide **7**

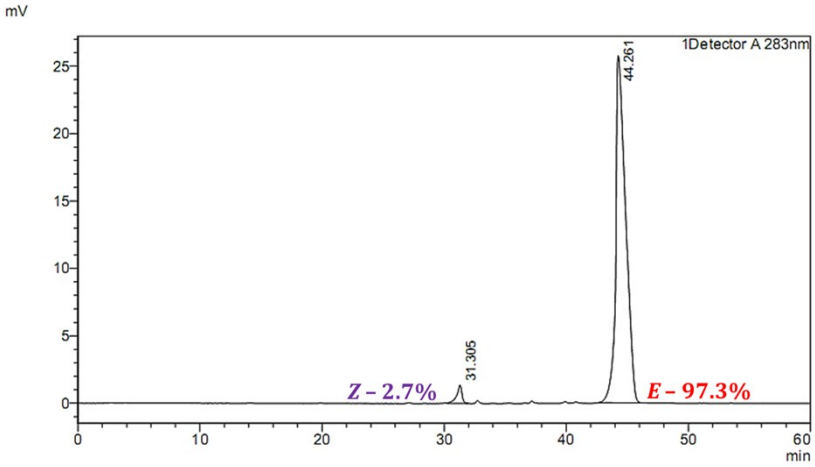

(g) azo-peptide **8**

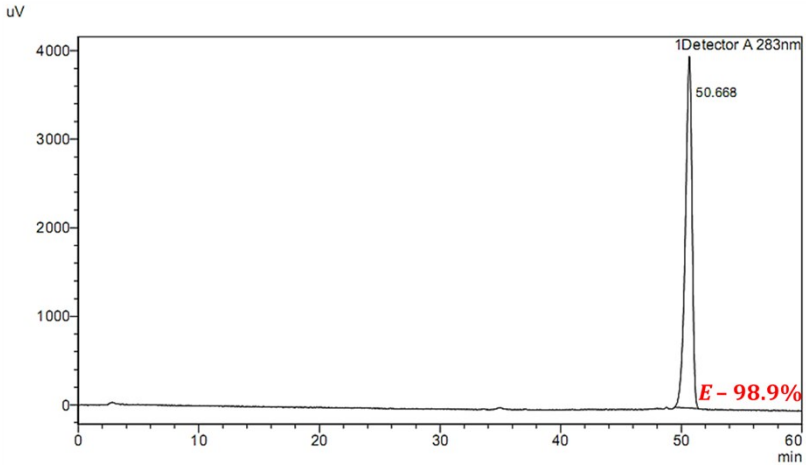

(h) azo-peptide **9**

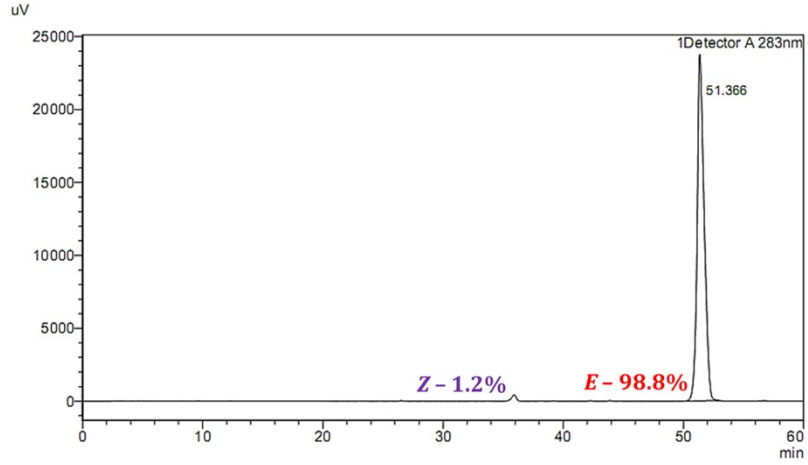

(i) azo-peptide **10**

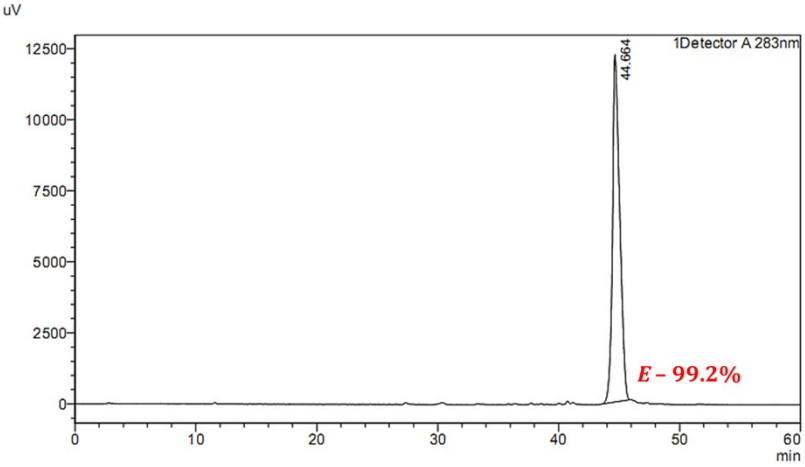

(j) azo-peptide **11**

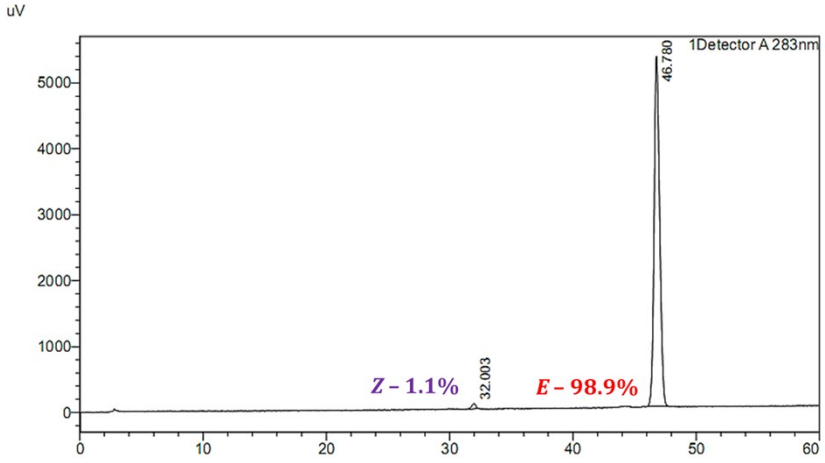

(k) azo-peptide **12**

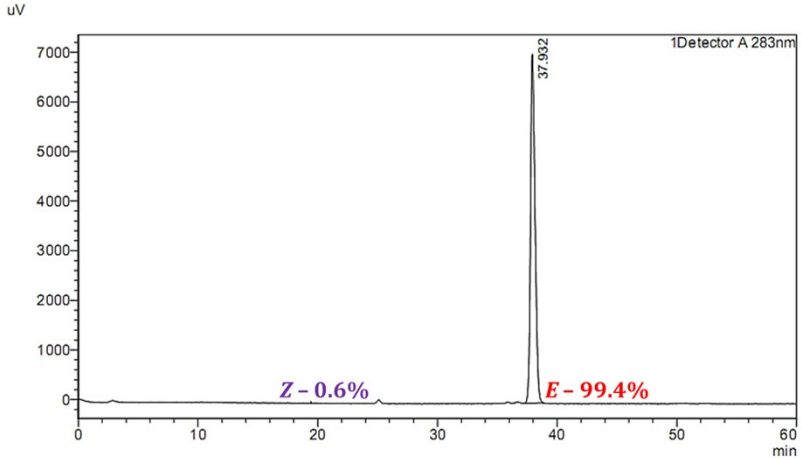

(l) azo-peptide **13**

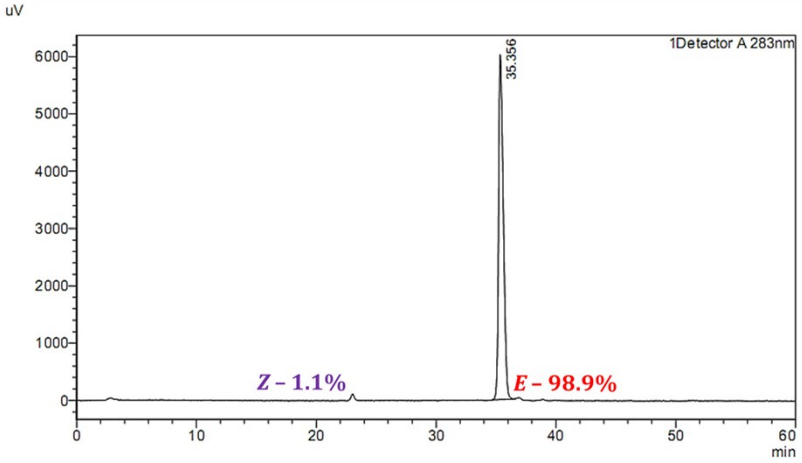

(m) azo-peptide **14**

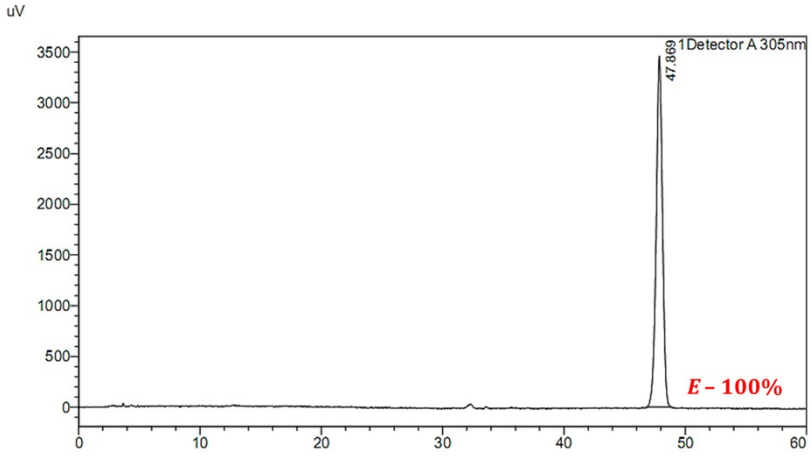

(n) azo-peptide **15**

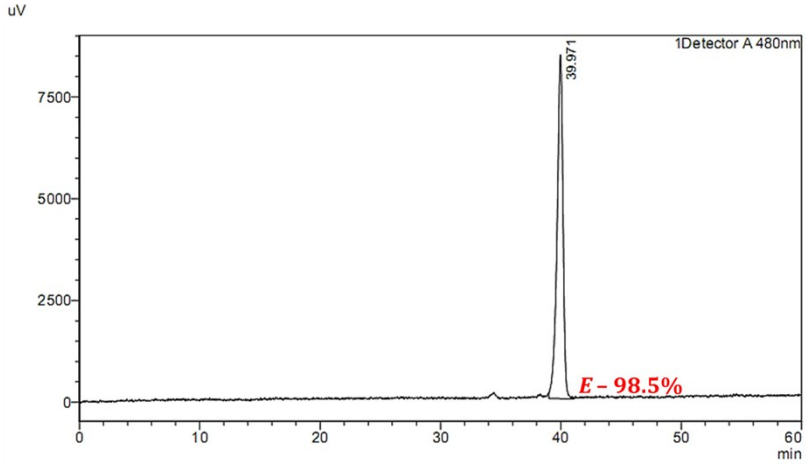

(o) azo-peptide **16**

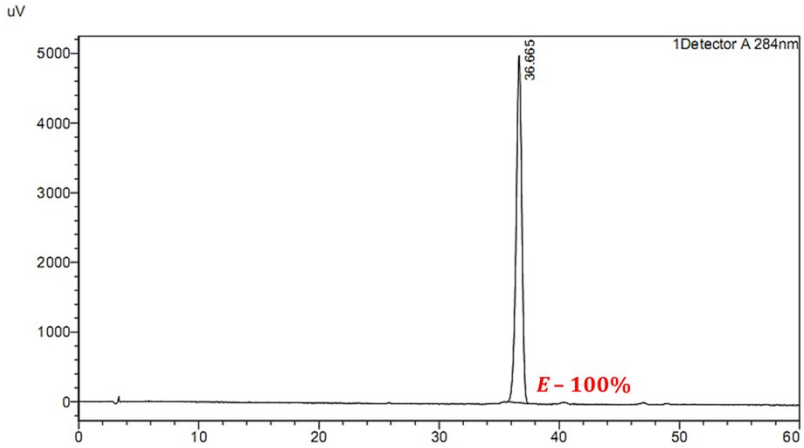

(p) azo-peptide **17**

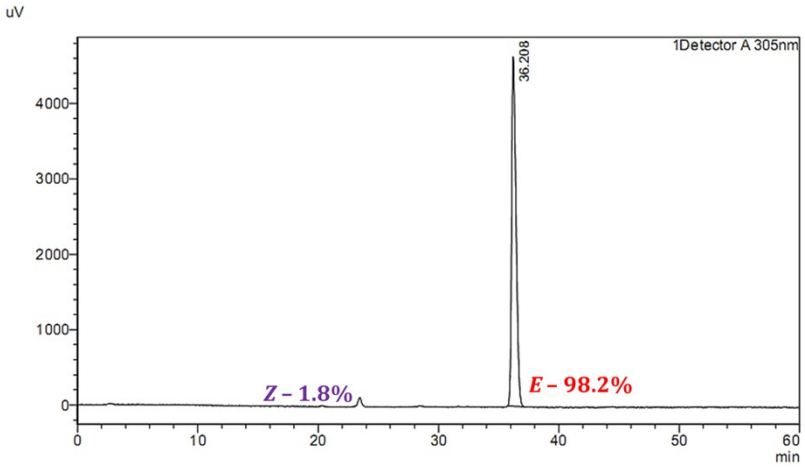

Figure S17. HPLC chromatograms are showing > 95% purity. Conditions of the RP-HPLC analysis; Column - $5C_{18}$-MS-II, 4.6×250 mm (Nacalai Tesque, Inc.); Eluent - CH_3CN/H_2O containing 0.1% TFA; Solvent gradient - 20 to 45% of acetonitrile in water for 1 h; Flow rate - 1 mL/min. Injection volume - 20 µL was used to analyze the purity of each azo-peptide.

3. Photoisomerization of the azo-peptides:

Photoisomerization experiments of compounds **11**, **14**, **15**, **16** were performed in BRB-80 buffer at 25 °C.

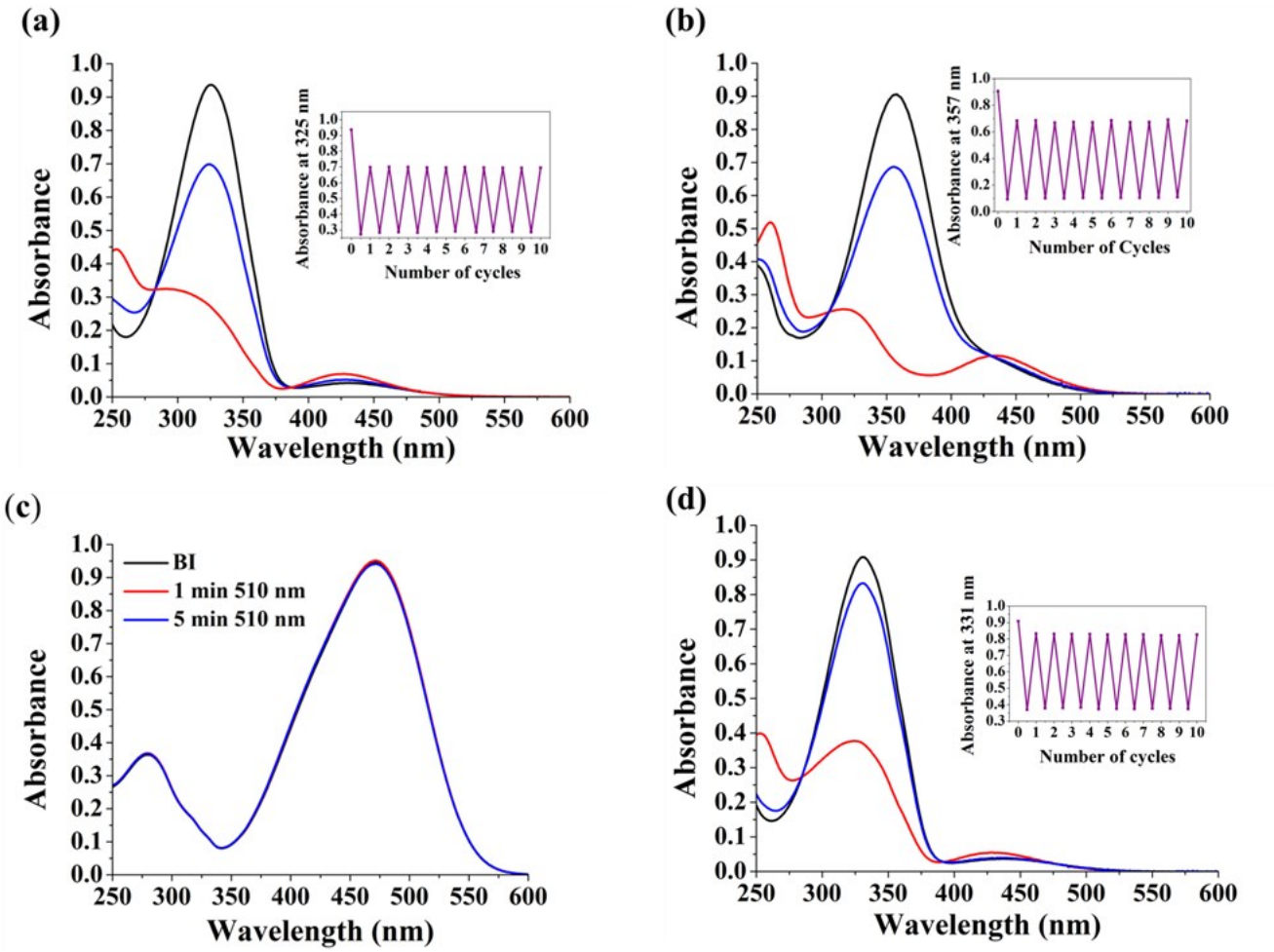

Figure S18. (a), (b), (c) and (d) are the UV-Vis absorption spectra of azo-peptides **11**, **14**, **15** and **16** respectively in BRB-80 buffer solution at 25 °C; before irradiation (black line), UV PSS (red line), Vis PSS (blue line). Inset of (a), (b), and (d): Absorbance changes at 325 nm, 357 nm and 331 nm respectively after the alternate irradiations of 365 and 436 nm for azo-peptides **11** and **16**, 365 and 510 nm for azo-peptide **14** for 10 cycles. Azo-peptide **15** was irradiated with 510 nm light.

4. Thermal stability of the *cis* isomers:

Thermal stability studies of the *cis* isomers of azo-peptides **14** and **16** were performed in BRB-80 buffer at 25 °C.

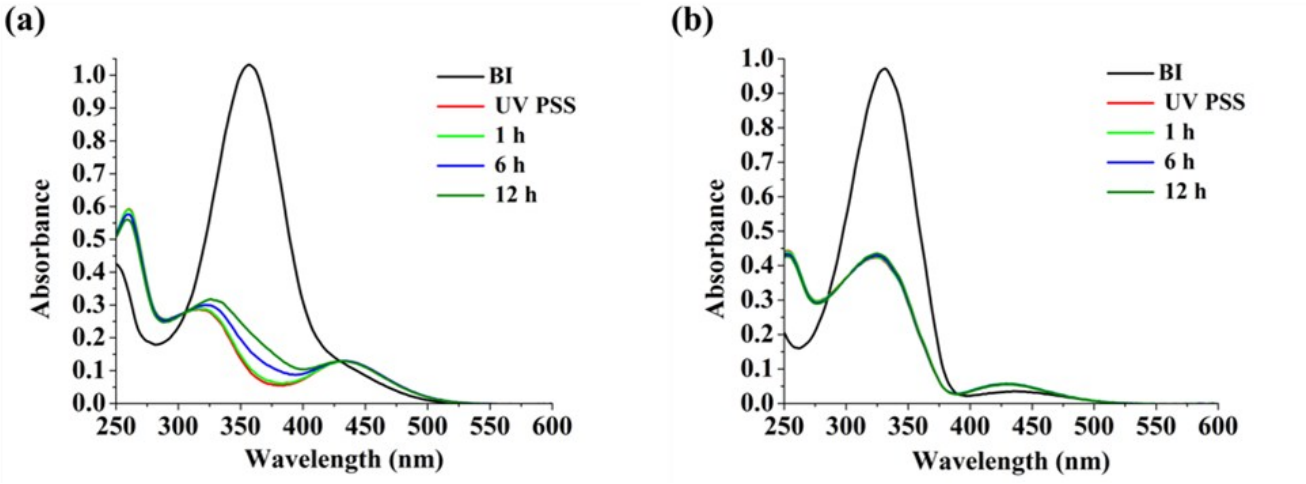

Figure S19. UV-Vis absorption spectra of azo-peptides **14** and **16** showing their thermal stability in BRB-80 buffer solution are represented by (a) and (b) respectively after irradiating with 365 nm light up to their PSSs and then incubation in the dark at 25 °C.

5. HPLC analysis on the conversion ratio from *trans* to *cis* and *cis* to *trans* forms:

The photo conversion ratio from *trans (E) to cis (Z) and cis (Z) to trans (E)* of the azo unit in azo-peptides **11**, **14** and **16** upon irradiation with 365 nm light and 436 nm or 510 nm light was measured with HPLC analyses. Conditions of the RP-HPLC analysis; Column - $5C_{18}$-MS-II, 4.6×250 mm (Nacalai Tesque, Inc.); Eluent - CH_3CN/H_2O containing 0.1% TFA; Solvent gradient - 20 to 45% of acetonitrile in water for 1 h; Flow rate – 1 mL/min. Injection volume -20 µL was used to analyze the isomer ratio and the isosbestic point in this eluent condition (283 nm for **11**, 305 nm for **14**, 284 nm for **16**) was used as the monitoring wavelength.

(a) azo-peptide **11**

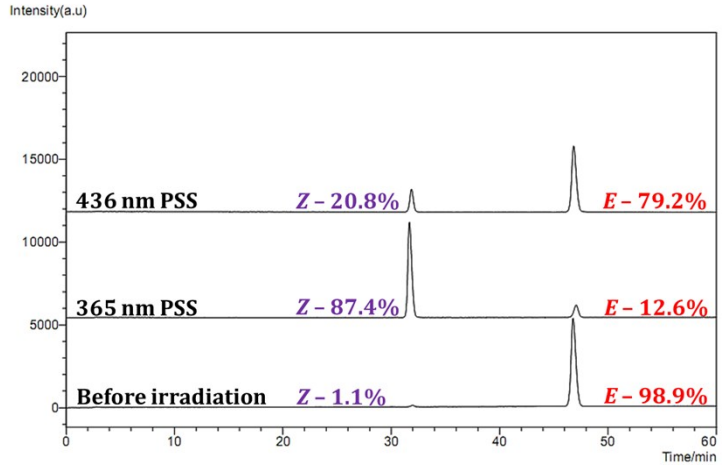

(b) azo-peptide **14**

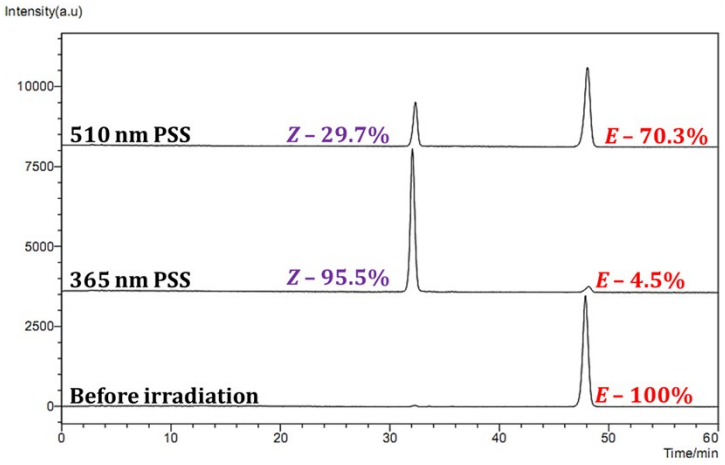

(c) azo-peptide **16**

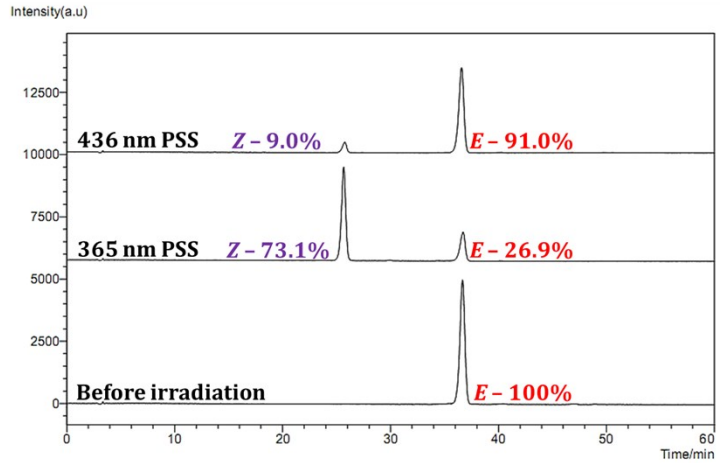

Figure S20. HPLC chromatograms showing the *cis* (*Z*) and *trans* (*E*) isomer ratio at before irradiation, after 365 nm light irradiation at PSS and after 436 nm or 510 nm light irradiation at PSS.

6. Structural comparison between the *Drosophila melanogaster* kinesin-1 and human kinesin-1 motor domains

(a)

(b)

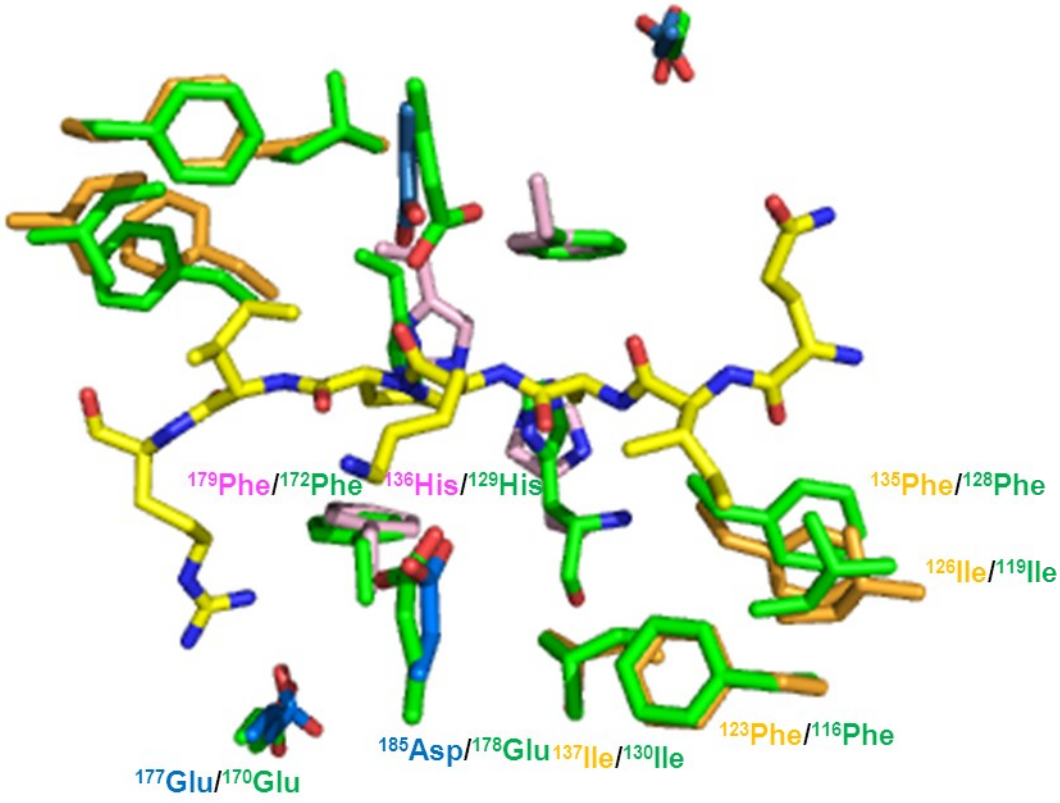

Figure S21. (a) Overlay of *Drosophila melanogaster* kiensin-1 (gray, PDB: 2Y65) and human kinesin motor domains (green, PDB: 1BG2). (b) Detailed similarity in critical amino acids for tail binding.